

# Field-induced local moments around nonmagnetic impurities in metallic cuprates

M. Gabay<sup>1</sup>, E. Semel<sup>1</sup>, P.J. Hirschfeld<sup>2</sup> and W. Chen<sup>2</sup>

<sup>1</sup>*Laboratoire de Physique des Solides, Univ Paris-Sud, UMR 8502, F-91405 Orsay France*

<sup>2</sup>*Department of Physics, University of Florida, Gainesville, FL 32611 USA*

We consider a defect in a strongly correlated host metal and discuss, within a slave boson mean field formalism for the  $t - t' - J$  model, the formation of an induced paramagnetic moment which is extended over nearby sites. We study in particular an impurity in a metallic band, suitable for modelling the optimally doped cuprates, in a regime where the impurity moment is paramagnetic. The form of the local susceptibility as a function of temperature and doping is found to agree well with recent NMR experiments, without including screening processes leading to the Kondo effect.

(February 2, 2008)

PACS numbers:

## I. INTRODUCTION

The remarkable character of disorder effects in low-dimensional, strongly correlated materials, has been emphasized in recent work on these systems (for a review, see Ref. 1). Doping a Mott insulator usually involves atomic substitutions which generate random electric potentials in the material and frequently structural changes as well; these defects induce large scale perturbations very different from analogous defects in noninteracting systems. Early studies of cuprate high temperature superconductors (HTSC)<sup>2,3,4</sup> led to the discovery that non-magnetic point defects (typically Zn, Li defects) enhance local AF correlations over a wide range of temperatures and dopings. substituting Cu atoms in the CuO<sub>2</sub> planes. Defects produced by electron irradiation also appear to produce very similar physical effects as Zn and Li in many cases<sup>1</sup>. Nuclear magnetic resonance (NMR) spectroscopy revealed the main features of this impurity-driven magnetic polarization in the normal (N) and superconducting (S) states of underdoped (UD), optimally doped (OP), and overdoped (OD) YBCO samples. In the presence of a uniform field  $B$ , a staggered magnetization (SM) pattern due to moments on the Cu(2) ions is formed around the impurity, with a spatial extent  $\xi$ , related to the correlation length of the pure system. This highly correlated, dynamic entity produces a paramagnetic polarizability  $\delta\chi$  which is Curie-like in the UD system, evolving to Curie-Weiss-like behavior  $\delta\chi \sim (T + \Theta)^{-1}$  in the OP to OD range<sup>4</sup>. Although these were controlled experiments on systematic impurity substitutions for Cu, it is important to realize that similar magnetic phenomena are to be expected to occur for intrinsic disorder due to the doping process itself, and may dominate some of the low-frequency properties of most cuprate samples, particularly in the UD regime.

Because  $\Theta$  increases rapidly with doping, and because resistivity measurements show that these defects cause very rapid scattering at low  $T$ , it has sometimes been interpreted as a Kondo temperature, enhanced in the presence of higher carrier densities capable of screening the

magnetic moment induced by the impurity<sup>4</sup>. Several observations are at odds with a simple Kondo picture: magnetic and transport signatures are quite strong above  $\Theta$  in the UD regime;  $\xi$  is considerably larger than the lattice spacing; the amplitude of the SM is much bigger than what one would expect from the Friedel response to a Kondo screened moment.

The problem of a single nonmagnetic impurity in a correlated host material has already received considerable theoretical attention. In the weak-coupling limit, several authors<sup>5,6,7,8,9</sup> modelled the problem with a localized potential added to a Hubbard Hamiltonian treated in a Hartree-Fock approximation. They used NMR and transport data for the pure system to assign values to the parameters of the model, and obtained good agreement between theory and experiment for impurity Knight shifts (in the N and S states) and resistivities (in the N state)<sup>10</sup> if the Hubbard  $U$  was tuned to a value quite close to a long range AF instability and if the impurity potential was chosen to be nonlocal in the N state. The strong coupling,  $U \rightarrow \infty$ , limit was considered along two main lines. One assumes that a magnetic moment has formed as a result of the impurity and the Kondo-screening response of the correlated medium is then studied<sup>11,12</sup>. The other approach models the pseudogap in the UD regime, and finds an induced SM (a spinon boundstate) around the impurity<sup>13,14</sup>. The problem has also been studied in essentially numerical treatments<sup>15,16,17,18</sup>.

In this letter, we provide a semiquantitative solution to the problem of a single pointlike, nonmagnetic impurity in the OP to OD regimes, with negligible pseudogap, i.e. in the metallic N state of a strongly correlated material described by the  $t - t' - J$  model. Within a mean field slave-boson formalism, appropriate to the  $U \rightarrow \infty$  limit, we derive the set of equations describing the paramagnetic moments on the planar Cu sites created by a uniform magnetic field. We give an approximate analytical solution to these equations which allows us to capture the physics at play: a resonant state is formed, producing a spatial SM pattern. Its amplitude, which is related to the staggered response of the pure system, can be quite large but it decays spatially as one moves a few lattice spacings

away from the impurity. The local polarizability  $\delta\chi$  has a Curie-Weiss form with a  $\Theta$  that depends sensitively on doping. The widths of the spinon and holon bands decrease significantly as one moves towards the impurity, suggesting a local near-critical region in the vicinity of the defect. These results are qualitatively corroborated by a fully self-consistent numerical solution of the equations. The formation of these moments and their screening by the correlated medium stem from the same set of carriers, in contrast with the standard Kondo scenario.

## II. HOMOGENEOUS MODEL.

Our starting point is the  $t - t' - J$  model on a square lattice, which is commonly considered to capture the low energy physics of the  $\text{CuO}_2$  plane common to all cuprate materials. The additional constraint of non double occupancy of the sites is handled via the slave boson formalism in which a projected fermion is represented by a product of auxiliary (“slave”) fields. The Hamiltonian of the impurity-free system in the presence of an applied magnetic field  $B$  then reads<sup>19,20</sup>

$$\mathcal{H} = - \sum_{\langle i,j \rangle \sigma} t_{ij} b_i^\dagger b_j^\dagger f_{i\sigma}^\dagger f_{j\sigma} - \frac{g\mu_B B}{2} \sum_{\sigma} \sigma f_{i\sigma}^\dagger f_{i\sigma} \quad (1)$$

$$+ \sum_{\langle i,j \rangle} J (\vec{S}_i \cdot \vec{S}_j - \frac{1}{4} n_i n_j) - \mu_0 \sum_{i\sigma} f_{i\sigma}^\dagger f_{j\sigma}$$

It describes strongly correlated fermions  $c_{i\sigma}^\dagger = b_i f_{i\sigma}^\dagger$  ( $b_i$  are bosons (holons) and  $f_{i\sigma}^\dagger$  are pseudo-fermions with spin  $\sigma$  (spinons)) on a square lattice, with hopping amplitudes  $t$  ( $t'$ ) between nearest- (next-nearest-) neighbor sites and nearest-neighbor antiferromagnetic interactions  $J$  between spins represented by  $\vec{S}_i = \frac{1}{2} f_i^\dagger \cdot \vec{\sigma} \cdot f_i$ . The fields are subjected to a local constraint  $\sum_{\sigma} n_{i\sigma} + b_i^\dagger b_i = 1$  ( $n_{i\sigma} = f_{i\sigma}^\dagger f_{i\sigma}$ ) which projects out double occupancy from the Hilbert space; it is enforced in the functional form of Eq. (1) with Lagrange multipliers  $\lambda_i$

We use a variant of Ubbens and Lee’s<sup>21</sup> mean field decoupling scheme, appropriate to the gapless spin liquid regime when magnetic solutions are included, and introduce the order parameters:

$$\begin{aligned} \langle f_{i\sigma}^\dagger f_{j\sigma} \rangle &= \chi_{ij} & \langle S_i^z \rangle &= m_i \\ \langle b_j^\dagger b_i \rangle &= Q_{ij} & \sum_i \langle b_i^\dagger b_i \rangle &= N\delta, \end{aligned} \quad (2)$$

where the last expression implements the local constraint on the average, and has been given in terms of the average hole doping per site  $\delta$ . The functional form of the resulting Lagrangian for the Bose ( $b$ ) and for the Grassmann ( $f$ ) fields and the phase diagram determined in this approximation are given in Ref. 21.

The homogeneous paramagnetic normal state is obtained with the choices

$$\chi_{ij} = \chi, Q_{ij} = Q, m_i = m = \frac{g\mu_B B \chi_0}{1 + 4J\chi_0}, i\lambda_i = \Lambda, \quad (3)$$

yielding a uniform stationary Lagrangian  $\mathcal{L}_0(\chi, Q, \Lambda)$  ( $\chi_0$  is the non interacting Pauli susceptibility for the renormalized spinon band). Correlations affect the effective bandwidths of the particles carrying spin and charge. In the homogeneous case, these bands reduce to

$$\epsilon_{\mathbf{k}}^{f,b} = -2t_{f,b}(\cos k_x + \cos k_y) + 4|t'_{f,b}| \cos k_x \cos k_y \quad (4)$$

with  $t_f = (J/2)\chi + tQ$ ,  $t'_f = t'Q'$ ,  $t_b = 2t\chi$ , and  $t'_b = 2t'\chi'$ . Unprimed and primed variables refer to nearest and next nearest neighbor amplitudes, respectively.

## III. SEMIANALYTICAL CALCULATION OF LOCAL MAGNETIZATION NEAR IMPURITY

We now assume the presence a single impurity, e.g. a zinc atom. Since  $\text{Zn}^{++}$  has a filled shell, there are no spinons and no holons. We model this by adding a term to Hamiltonian (1) that effectively projects out site 0,

$$\lambda \left( \sum_{\sigma} f_{0\sigma}^\dagger f_{0\sigma} + b_0^\dagger b_0 \right) \quad (5)$$

with  $\lambda \rightarrow \infty$ . In mean field, the charge and spin sectors can be studied separately, and we denote by  $\mathcal{G}^b$  ( $\mathcal{G}_\sigma$ ) the Green functions for the holons (spinons) species with the  $\lambda$  perturbation, when  $B$  is present. If an impurity-induced magnetic polarization develops in the system, with site dependent magnetizations  $m_i \neq m$  (see Eqs. (2,3)), we need to include processes due to this magnetic scattering potential. It can be written as  $V = \sum_{\sigma} V_{\sigma} = J \sum_{\langle i,j \rangle \sigma} (m_j - m) \sigma n_{i\sigma}$  if we replace  $B$  by  $B_M = B - \frac{4Jm}{g\mu_B}$ . The full spinon Green’s function  $G_\sigma$  is then formally given by

$$G_\sigma = \mathcal{G}_\sigma + \mathcal{G}_\sigma V_\sigma G_\sigma, \quad (6)$$

which gives a self-consistent set of equations for the magnetizations

$$m_i = -\frac{1}{\pi} \text{Im} \int d\omega f(\omega) \sum_{\sigma} \sigma G_\sigma(i, i; \omega), \quad (7)$$

where  $f$  is the Fermi function. In the paramagnetic regime, this gives us the linear response to the applied field  $B$  in the form

$$\sum_j M_{ij} s_j = \frac{-\text{Im} \int \frac{d\omega}{\pi} f'(\omega) \left( \mathcal{G}(i, i; \omega) - G^0(i, i; \omega) \right)}{-\text{Im} \int \frac{d\omega}{\pi} f'(\omega) G^0(i, i; \omega)}, \quad (8)$$

where both  $\mathcal{G}$  and  $G^0$  (the Green's function of the defect-free problem) are spin-independent in zero field,  $s_j = (m_j - m)/m$  and  $M_{ij} = \delta_{ij} - \frac{1}{2}J \sum_k - \frac{1}{\pi} \text{Im} \int d\omega f(\omega) \left( \mathcal{G}(i, k; \omega) \mathcal{G}(k, i; \omega) \right)$  ( $k$  and  $j$ ,  $i$  and  $j$  are nearest-neighbors). The stability of a paramagnetic solution requires that all the eigenvalues of the matrix  $\mathbf{M} = (M_{ij})$  be strictly positive. In order to determine the  $s_i$  we need to determine  $\mathcal{G}^b, \mathcal{G}$ . Since Eq. (5) describes the removal of the site 0, the solution in the case of a rigid band would be

$$\mathcal{G}(i, j) \xrightarrow{\lambda \rightarrow \infty} G^0(i, j) - \frac{G^0(i, 0)G^0(0, j)}{G^0(0, 0)} \quad (9)$$

and a similar form for  $\mathcal{G}^b$ . However, Eq. (2) shows that  $\chi_{ij}$ ,  $Q_{ij}$  are site dependent, whereas Eq. (3) holds only for the homogeneous system. Preserving self-consistent determinations of these parameters implies including scattering potentials proportional to  $\chi_{ij} - \chi$  and  $Q_{ij} - Q$  in the Dyson equations for  $\mathcal{G}^b, \mathcal{G}$ . Enforcing the non double occupancy constraint also requires special care. A full solution for these propagators involves a numerical calculation (see below).

Nevertheless, using perturbation theory and controlled approximations, we obtain an analytical solution which reveals the nature and main features of the induced polarization. To zeroth order, we use Eq. (9) which allows us to compute the densities of states and to determine  $\chi_{ij}$ ,  $Q_{ij}$  in Eq. (2). On sites close to the impurity, the potential Eq. (5) pushes states away from the edges of the band (Eq. (4)) and redistributes those inside the band. Holons, which sit primarily at the bottom of the band are drastically affected, and  $Q_{ij}$  is strongly suppressed.  $\chi_{ij}$  almost retains its defect-free value, since its main contribution comes from spinons at the Fermi level, well inside the band. Beyond a characteristic "healing length" these parameters recover their unperturbed values. We then use these values of  $Q_{ij}$  and  $\chi_{ij}$  to generate the Green functions  $\mathcal{G}^b, \mathcal{G}$  to next order in perturbation. We do not iterate the process any further, which implies that, within the healing length, we do not obtain the bond order parameters in a self-consistent manner and that the non double occupancy constraint is not enforced properly. Yet, this truncation, which allows us to handle analytically tractable expressions, is not too drastic a simplification, for two reasons. One is that, for temperatures comparable to or larger than  $\Theta$ , this healing length is quite small, as is seen in Fig. 1, which shows the local spinon bandwidth at site  $i$ ,  $t_f(i)$ , as a function of the distance  $r_i$  from the impurity. The second is that at all  $T$ , the amplitude of induced staggered polarization decays very quickly with  $r_i$ , and we may consider that the system settles back into the unperturbed state for  $r_i$  larger than  $\xi$  (Fig. 2) of order a few lattice spacing.

Using these approximations, we solve Eq. (8), where we consider that the only nonzero  $s_i$  are for sites  $i$  sitting up to three shells away from the impurity. We noticed (see below) that the integral in the expression for  $M_{ij}$

is proportional to  $J/t_f(i)$ , and the enhancement close to the impurity promotes a tendency towards local moment formation, i.e. sizable values of the  $s_i$ . Far from the impurity, this ratio is much smaller and the magnitude of the impurity-induced polarization  $s_i$  goes to zero. Values ascribed to the hopping and correlation amplitudes were  $t = 0.45\text{eV}$ ,  $t' = -0.4t$ ,  $J = 0.1\text{eV}$ , and the field was set to  $B = 7\text{T}$ . The measured values of the Knight shifts for the pure system and their  $\delta$  and  $T$  variations were well reproduced if we assign a value  $\delta = 0.3$  to the hole concentration at optimal doping. Experimentally, optimal doping corresponds to  $\delta = 0.15$  rather than 0.3. A plausible reason which explains this difference is that we are using a mean field decoupling. Nevertheless, with our choice of parameters we get a value of the homogeneous  $t_f$  Eq. (4) extremely close to that determined in the framework of a projected Gutzwiller scheme, where the doping is set to 0.16<sup>22,23,24,25</sup>. As we pointed out, the large amplitudes of the staggered moments near the impurity appear to correlate with the ratios  $J/t_f(i)$ . Indeed, the observed reduction of  $t_f$  compared to the homogeneous case, for sites close to the impurity, has two main impacts. One is to create an extended effective scattering potential, and this enhances the weight of the staggered Fourier component of the local paramagnetic magnetizations  $m_i$ . The other is to increase the magnetic response<sup>26</sup>, since – in a Stoner-like picture – a larger value of  $J/t_f(i)$  brings the system locally closer to a magnetic phase. It is noteworthy that in the range of dopings and temperatures that we investigated, the smallest eigenvalue of  $\mathbf{M}$  decreases as one decreases  $\delta$  and is always more than one order of magnitude smaller than the others, which are of order 1. Since it is positive, this confirms that the induced magnetization vanishes in zero field. Its smallness indicates a resonant state, close to a transition to a bound state, but the accuracy of the calculation does not allow one to make a stronger statement. It also shows that in the absence of the impurity, where  $\mathcal{G} \equiv G^0$ , the only solution to Eq. (8) is  $s_i = 0$ , for all  $i$ . A numerical inspection of the sum over  $k$  in the expression of  $M_{ij}$  reveals that the dominant contribution is obtained when  $k = i$ , and that the integration of this term over  $\omega$  is proportional to  $1/t_f(i)$ .

In order to give a functional expression for the staggered polarization, we have sought to fit the solution of Eq. (8) with a form

$$s_i = (-1)^{x_i+y_i+1} s_1(T, \delta) f\left(\frac{\mathbf{r}_i}{\xi(T, \delta)}\right) g(\mathbf{q} \cdot \mathbf{r}_i) \quad (10)$$

for a site at position  $\mathbf{r}_i = (x_i, y_i)$  away from the impurity. The factor  $g(\mathbf{q} \cdot \mathbf{r}_i) = 0.5(\cos(\pi q x_i) + \cos(\pi q y_i))$  allows us to include both commensurate ( $q = 0$ ) and incommensurate solutions. We found that the best fit to the data was obtained for a commensurate modulation, when we chose for  $f(x_i, y_i)$  the (square) lattice version of the Bessel function  $K_0$ , normalized to a nearest neighbor distance (Fig. 2). This is not a form which emerges analytically from the current theory, but rather one mo-

tivated by rigorous theories for similar problems in 1D<sup>1</sup>. Note that according to Ref.27, apart from the underdoped regime,  $m$  does not vary significantly with  $T$ , so one may use the above fitting form either for the  $s_i$  or for the  $(m_i - m)/B$ .

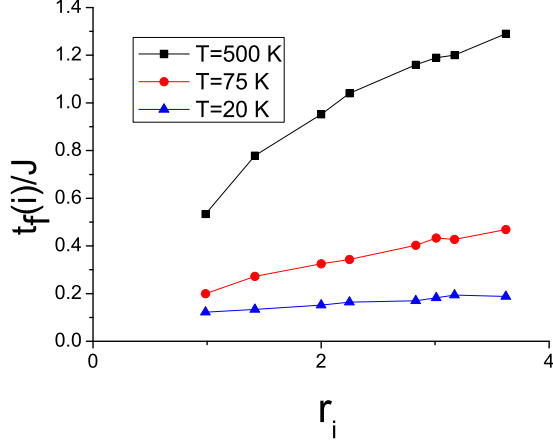


FIG. 1: Local spinon bandwidth  $t_f(i)$  in units of  $J$ , as a function of the distance from the impurity site  $r_i$  in lattice constants at different temperatures, for  $\frac{J}{t} = 0.22$ ,  $\delta = 0.3$ .

The relative polarization  $s_1(T)$  is well represented by a Curie-Weiss form  $C/(T + \Theta)$ , as found in experiment. The magnitude of  $s_1$  is strongly enhanced compared to what we would have found as a result of a standard Friedel oscillation (the solution of Eq. (8) when one sets  $J = 0$  in the definition of the  $M_{ij}$ ). Let us emphasize once again that these features are direct consequences of the correlation term  $\frac{J}{t_f(i)}$  and that they are strikingly similar with those found in 1D for the case of a non-magnetic impurity<sup>1</sup>. Our analytic solution allowed us to determine  $C$ ,  $\Theta$  and  $\xi$  for  $\delta = 0.28, 0.3, 0.32$  and the results are summarized in the plots of Fig. 2.

#### IV. FULLY SELF-CONSISTENT EVALUATION

One uncertainty in the above discussion involves the fact that while the system with impurity is electronically inhomogeneous, the slave boson constraint has only been enforced globally. To check the accuracy of this approximation, we perform real space exact diagonalization of Eq. (1), plus the impurity potential (5), solved together with the self-consistently determined local slave boson amplitudes<sup>16,28,29,30</sup>. The primary effect of the constraint, which we now impose locally, appears to be to slave the spatial variation of the holon density to that of the spinons, and thus eliminate the unphysical free bosonic length scale. In fact, the effects of correlations are generally mitigated, e.g. the normalized staggered magnetization is also reduced relative to Fig. 2. We find

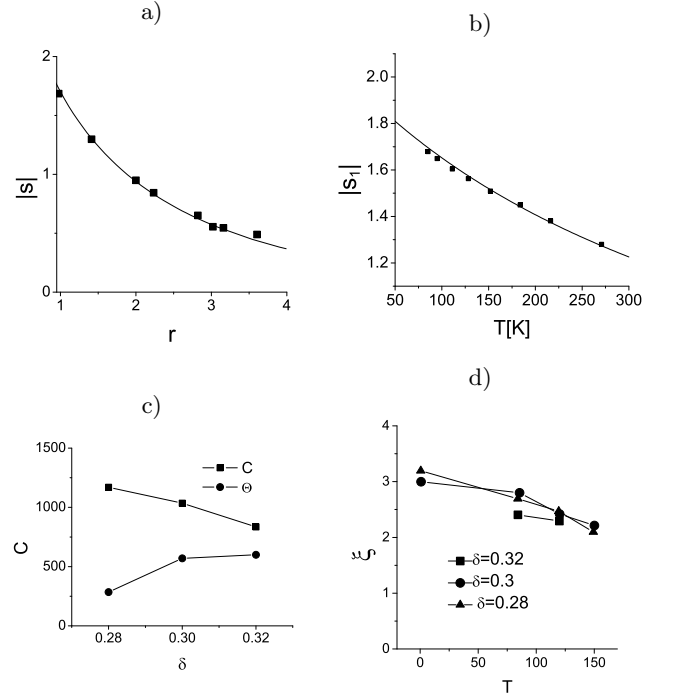


FIG. 2: Normalized staggered magnetization  $s(r) \equiv (m(r) - m)/m$  induced by a nonmagnetic impurity in the  $t - t' - J$  model in the presence of a magnetic field  $B$  of 7 Tesla, where  $m$  is the magnetization of the homogeneous system induced by the field. a) normalized magnetization  $|s|$  near impurity at  $T = 25\text{K}$  for  $J/t = 0.22$  and  $\delta = 0.3$ . Solid line: fit to  $|s(r)| \propto s(1)K_0(r/\xi)/K_0(1/\xi)$  for  $\xi = 3$ . b)  $T$ -dependence of nearest-neighbor normalized magnetization  $s_1$  for same parameters. c) Effective moment  $C$  and Curie-Weiss temperature  $\Theta$  vs. doping  $\delta$ . d) correlation length  $\xi$  vs.  $T$  extracted from fit illustrated in (a).

that the results of the fully self-consistent evaluation appear to agree qualitatively with those of the semianalytic approach, but for a smaller, more realistic doping scale.

Fig. 3 shows the reduction of  $t_f$  in the vicinity of the impurity. It is qualitatively similar to that found using the analytic approach, (Fig. 1) but we notice differences between the two results. In the fully self-consistent calculation, both the spinon bandwidth healing length – which has a smaller value than that given by the analytic calculation – and  $t_f(i)$  are temperature independent. This is a direct consequence of the enforcement of the constraint. Holons are slaved to spinons and the spatial variations of  $Q_{ij}$  and  $\chi_{ij}$  with  $r_i$  depend on one single characteristic (renormalized Fermi) energy. By contrast, in the analytic calculation, holons are treated as quasi-free bosons and so the spatial variations of  $Q_{ij}$  depend on  $k_B T$  while those of  $\chi_{ij}$  are set by the spinon Fermi energy, which is proportional to the homogeneous  $t_f$ . For experimentally relevant temperatures,  $k_B T \ll t_f$ , and so the spatial variations of  $t_f(i)$  track mainly those of the holons.

In Fig. 4, we show results of the full evaluation which

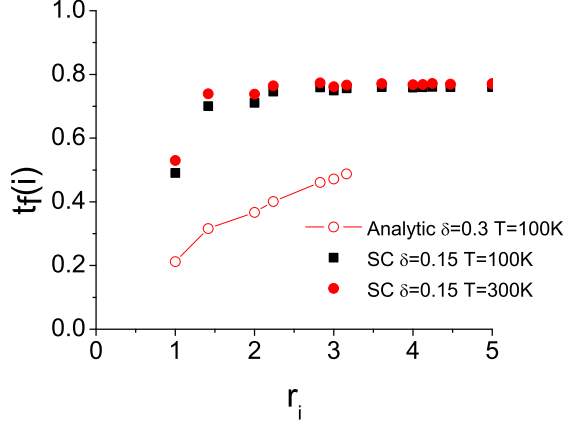


FIG. 3: Spinon bandwidth in fully self-consistent evaluation as a function of distance from the impurity site at filling  $\delta = 0.15$  and  $T = 100K$  (filled squares) and  $300K$  (filled circles). Bandwidth from semianalytic calculation at  $\delta = 0.3$  and  $100K$  is shown (open circles) for comparison.

again reproduce the qualitative aspects of experimental NMR results on Zn and Li impurities. In Fig. 4a, we show the magnetization on the nearest neighbor site in an applied 7T field. The low-temperature upturn of this magnetization increases in strength as the doping is lowered. It is important to recall that in the mean field treatment of the homogeneous system, there is a transition to long range antiferromagnetic order as the temperature and filling are lowered. Thus the enhanced upturns reflect the approach to this mean field transition, the best the mean field theory can do to simulate the gradual freezing of spin fluctuations in the underdoped phases, as documented, e.g. by NMR,  $\mu$ SR and neutron scattering expts.<sup>31,32,33,34,35,36,37,38,39</sup>

In each case, the upturn of the (normalized) magnetization on the nearest-neighbor site has been fit to a Curie-Weiss form, shown in the figure. The doping dependence of the prefactor  $C$  and the Weiss temperature  $\Theta$  are shown in Fig. 4b) respectively. Two types of terms control the  $T$  dependence of  $s_1$ . One is the Friedel-like response found in a normal metal, which is quasi- $T$ -independent and thus gives a constant  $s_1$  for  $T \gg \Theta$ . The other is the large, staggered response caused by a local reduction of  $t_f$ . It gives the main contribution to  $s_1$ , at intermediate  $T$  (larger than or comparable to  $\Theta$ ). For the lower dopings, the proximity to a magnetic phase affects the small  $T$  behavior. These factors modify the Curie-Weiss fit, and hence the ( $\delta$ -dependent) values of  $C$  and  $\Theta$ . Experimentally<sup>1,27</sup>,  $\Theta$  and  $C$  are obtained with sizable error bars near optimal doping, since  $\Theta$  varies rapidly with  $\delta$  in that range. Despite these limitations, a quite reasonable qualitative agreement is found between our results and those of Ref. 27 over the range of dopings where our theory applies. Below optimal doping, the

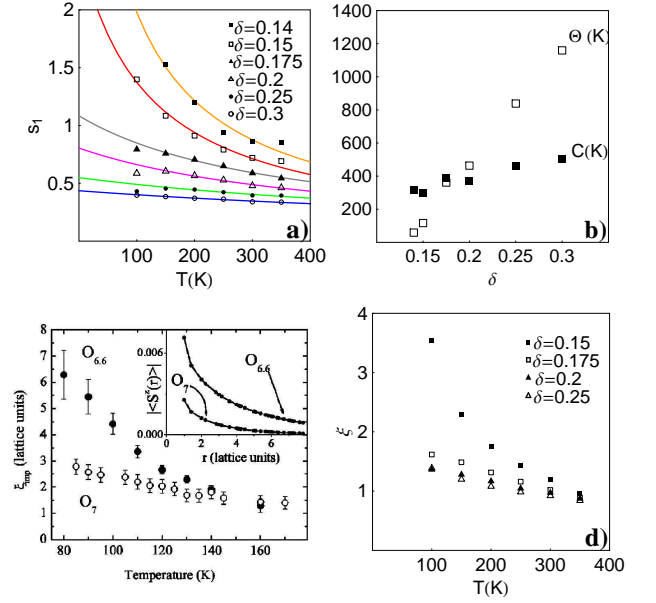


FIG. 4: Results for fully self-consistent evaluation of magnetization from slave boson equations. a) Normalized magnetization  $s_1$  on nearest-neighbor site as function of  $T$  for values of doping  $\delta$  from 0.14 to 0.30. Solid lines show fits to  $s_1 = C/(T + \Theta)$ . b) Effective moment constant  $C$  and Curie-Weiss constant  $\Theta$  extracted from fits in a) vs.  $\delta$ . c) Experimental data from Refs. 1,27, showing the magnetization  $\langle S_z \rangle$  vs. distance from impurity  $r$  (insert) and correlation length  $\xi$  vs.  $T$  extracted therefrom; d) Temperature dependence of extracted theoretical correlation lengths  $\xi$  vs.  $T$ .

current theory is not valid, since the pairing field which gives rise to the pseudogap in slave boson mean field is not present. As in the semianalytic calculations, the  $\Theta$  scale is somewhat larger than experiment around optimal doping; this may be due to the small pseudogap present even at optimal doping which is absent from the present theory. The pseudogap, as the superconducting gap itself, is known<sup>1</sup> to promote bound state formation and enhance the Curie behavior found in underdoped samples.

In Figs. 4c) and d), we show the spatial extent of the magnetic droplet which forms around the impurity compared with the results of Ref. 27; here too the agreement is fairly good. We note furthermore that the length scale extracted here is comparable with the antiferromagnetic correlation length of the defect-free system<sup>40,41</sup>, as found explicitly in 1D spin chains<sup>1</sup>. Finally, Fig. 5 shows the actual distribution of moments  $m_i$  on the various sites. Far from the impurity, this distribution tends to a finite value, since  $m_i \rightarrow m_0$  as  $r_i \rightarrow \infty$ . As the temperature is lowered further or the coupling  $J$  increased, the magnetization oscillations are enhanced further and the values on nearby sites of the same sublattice as the impurity actually take on negative values (not shown), as observed in experiment<sup>27</sup>. The reasonable agreement that is found

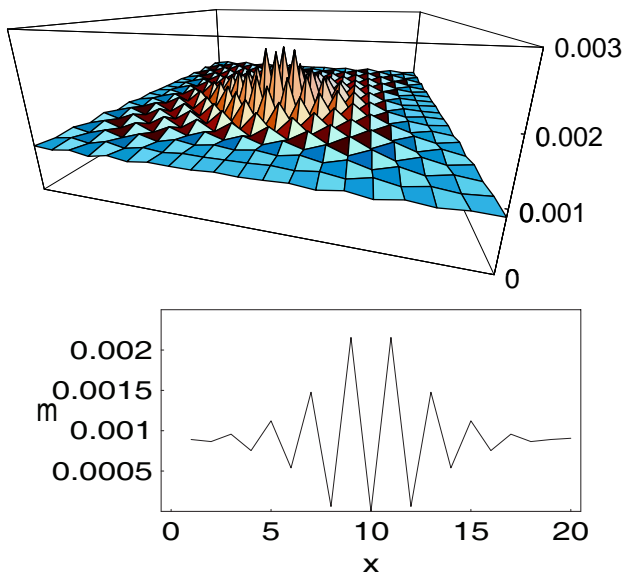


FIG. 5: Top: magnetization in real space obtained in fully self-consistent evaluation for  $\delta = 0.15$ ,  $B = 7T$  and  $T = 100K$ . Bottom: magnetization  $m$  cut through impurity site along  $x$  direction.

between the results of the semianalytical and numerical calculations (see Figs. 1-4) and experiment suggests that our approach contains key ingredients required to capture the physical mechanism of moment formation and screening in correlated systems.

## V. CONCLUSIONS

We have shown that a simple theory of a nonmagnetic impurity in a correlated host described by the slave boson mean field representation of the  $t - t' - J$  model can explain the basic features of the measured paramagnetic response of Zn impurities in YBCO. This theory differs from earlier approaches in that it explicitly treats the correlations in the strong coupling limit, yet assumes a metallic host suitable for discussion of optimal doping. The calculated susceptibility is found to be much stronger than the weak Friedel-like response expected for a normal metal, due not only to the enhanced background density of states in the host, but also to local suppression of the ef-

fective fermionic bandwidth around the impurity. Qualitatively, the impurity carves a hole around itself of size roughly the pure AF correlation length, and the response is therefore somewhat similar to that calculated earlier in models of the pseudogap state<sup>13,14</sup>; nevertheless, the temperature dependence is Curie-Weiss like, rather than Curie like, in agreement with experiment. The doping dependence is also found to be qualitatively in agreement with experiment, albeit with a renormalized doping scale. By utilizing a fully numerical treatment of the inhomogeneous slave boson problem, we have shown that the need for this renormalization arises primarily from an overestimation of the local bandwidth suppression due to the global enforcement of the slave boson constraint, which leads to an unphysical bosonic lengthscale. When the constraint is enforced locally, correlations are weaker and closer agreement with the realistic doping scale is obtained. The good qualitative agreement of the results in this work with experiment suggest that the screening of the moment reflected in the Curie-Weiss form of the susceptibility, which is observed to rise steeply as the system is doped, need not be due to many-body effects of traditional Kondo type. Instead, it arises from the correlation "hole" induced around the impurity by the Hubbard interaction, and can be captured by relatively simple mean field theories which ignore the spin-flip scattering which usually leads to Kondo physics. The cross section for quasiparticles scattered by the magnetic droplet created by the impurity is of course different for spins up and down; it is furthermore strongly  $T$ -dependent due not to Kondo screening but to the temperature dependence of the paramagnetic moment, as in 1D spin chains.

In principle, the slave boson approach is capable of capturing the entire crossover of the induced moment in a correlated host problem, from the metallic regime to pseudogap regime. To do this within a single formalism would be a useful step towards understanding the effects of disorder on the cuprate phase diagram, but requires the inclusion of pairing effects. Work along these lines is in progress.

*Acknowledgments.* PJH and WC were partially supported by ONR N00014-04-0060, DOE DE-FG02-05ER46236 and by visiting scholar grants from C.N.R.S. The authors are grateful to H. Alloul and J. Bobroff for many enlightening discussions and clarifications of experiments.

- 
- <sup>1</sup> H. Alloul, J. Bobroff, M. Gabay, and P. Hirschfeld, *cond-mat xxx* (2007).
  - <sup>2</sup> H. Alloul, P. Mendels, H. Casalta, J.-F. Marucco, and J. Arabshi, *Phys. Rev. Lett.* **67**, 3140 (1991).
  - <sup>3</sup> A. Mahajan, H. Alloul, G. Collin, and J. Marucco, *Phys. Rev. Lett.* **72**, 3100 (1994).
  - <sup>4</sup> J. Bobroff, W. MacFarlane, H. Alloul, P. Mendels, N. Blanchard, G. Collin, and J. Marucco, *Phys. Rev. Lett.* **83**, 4381

- (1999).
- <sup>5</sup> N. Bulut, *Phys. Rev. B* **61**, 9051 (2000).
- <sup>6</sup> Y. Ohashi, *J. Phys. Soc. Jpn* **70**, 2054 (2001).
- <sup>7</sup> N. Bulut, *Physica C* **363**, 260 (2001).
- <sup>8</sup> Y. Ohashi, *Phys. Rev. B* **66**, 054522 (2002).
- <sup>9</sup> J. W. Harter, B. M. Andersen, J. Bobroff, M. Gabay, and P. J. Hirschfeld, *Physical Review B* **75**, 054520 (2007).
- <sup>10</sup> H. Kontani and M. Ohno, *Phys. Rev. B* **74**, 014406 (2006).

- <sup>11</sup> G. Khaliullin and P. Fulde, Phys. Rev. B **52**, 9514 (1995).
- <sup>12</sup> W. Hofstetter, R. Bulla, and D. Vollhardt, Phys. Rev. Lett. **84**, 4417 (2000).
- <sup>13</sup> G. Khaliullin, R. Kilian, S. Krivenko, and P. Fulde, Phys. Rev. B **56**, 11882 (1997).
- <sup>14</sup> R. Kilian, S. Krivenko, G. Khaliullin, and P. Fulde, Phys. Rev. B **59**, 14432 (1999).
- <sup>15</sup> D. Poilblanc, D. Scalapino, and W. Hanke, Phys. Rev. B **50**, 13020 (1994).
- <sup>16</sup> W. Ziegler, D. Poilblanc, R. Preuss, and W. Hanke, Phys. Rev. B **53**, 8704 (1996).
- <sup>17</sup> S. Odashima and H. Matsumoto, Phys. Rev. B **56**, 126 (1997).
- <sup>18</sup> S. Odashima, H. Matsumoto, and O. Michikami, Physica C **336**, 287 (2000).
- <sup>19</sup> A. E. Ruckenstein, P. J. Hirschfeld, and J. Appel, Phys. Rev. B **36**, 857 (1987).
- <sup>20</sup> G. Baskaran, Z. Zou, and P. W. Anderson, Solid State Commun. **36**, 853 (1987).
- <sup>21</sup> M. Ubbens and P. Lee, Phys. Rev. B **46**, 8434 (1992).
- <sup>22</sup> F. Zhang and T. Rice, Phys. Rev. B **37**, 3759 (1988).
- <sup>23</sup> C. Shih, T. Lee, R. Eder, C.-Y. Mou, and Y. Chen, Phys. Rev. B **92**, 227002 (2004).
- <sup>24</sup> P. Anderson, P. Lee, M. Randeria, T. Rice, N. Triverdi, and F. Zhang (2004).
- <sup>25</sup> P. Lee, N. Nagaosa, and X. Wen, Rev. Mod. Phys. **78**, 17 (2006).
- <sup>26</sup> M. Gabay, Physica C **235-240**, 1337 (1994).
- <sup>27</sup> S. Ouazi, J. Bobroff, H. Alloul, and W. MacFarlane, Phys. Rev. B **70**, 104515 (2004).
- <sup>28</sup> W. Ziegler, H. Endres, and W. Hanke, Phys. Rev. B **58**, 4362 (1998).
- <sup>29</sup> J. Han and D.-H. Lee, Phys. Rev. Lett. **85**, 1100 (2000).
- <sup>30</sup> Z. Wang and P. Lee, Phys. Rev. Lett. **89**, 217002 (2002).
- <sup>31</sup> C. Niedermayer, C. Bernhard, T. Blasius, A. Golnik, A. Moodenbaugh, and J. I. Budnick, Phys. Rev. Lett. **80**, 3843 (1998).
- <sup>32</sup> Y. Sidis, C. Ulrich, P. Bourges, C. Bernhard, C. Niedermayer, L. P. Regnault, N. H. Andersen, and B. Keimer, Phys. Rev. Lett. **86**, 4100 (2001).
- <sup>33</sup> B. Lake, H.M.R. Onnnow, N. Christensen, G. Aeppli, K. Lefmann, D. McMorrow, P. Vorderwisch, P. Smeibidl, N. Mangkorntong, T. Sasagawa, et al., Nature **415**, 299 (2002).
- <sup>34</sup> C. Panagopoulos, J. L. Tallon, B. D. Rainford, T. Xiang, J. R. Cooper, and C. A. Scott, Phys. Rev. B **66**, 064501 (2002).
- <sup>35</sup> H. Kimura, M. Kofu, Y. Matsumoto, and K. Hirota<sup>2</sup>, Phys. Rev. Lett. **91**, 067002 (2003).
- <sup>36</sup> M.-H. Julien, Physica B **329-333**, 693 (2003).
- <sup>37</sup> C. Panagopoulos and V. Dobrosavljević, Phys. Rev. B **72**, 014536 (2005).
- <sup>38</sup> R. Miller, R. Kiefl, J. Brewer, Z. Salman, J. Sonier, F. Callaghan, D. Bonn, W. Hardy, and R. Liang, Physica B **374-375**, 215 (2006).
- <sup>39</sup> C. Stock, W. J. L. Buyers, Z. Yamani, C. L. Broholm, J.-H. Chung, Z. Tun, R. Liang, D. Bonn, W. N. Hardy, and R. J. Birgeneau, Physical Review B **73** (2006).
- <sup>40</sup> G. Aeppli, T. E. Mason, S. M. Hayden, H. A. Mook, and J. Kulda, Science **278**, 1432 (1997).
- <sup>41</sup> P. Bourges, in *The gap Symmetry and Fluctuations in High Temperature Superconductors*, edited by J. Bok, G. Deutscher, D. Pavuna, and S. Wolf (cond-mat/9901333, Proceedings of NATO ASI summer school held September 1-13, 1997 in Cargèse, 1998).